Materials Physics and Mechanics 42 (2019) 749-757 Received: April 16, 2018

ON WAVE FIELD FORMATION ON THE SURFACE OF PIEZOACTIVE BODIES WITH INHOMOGENEOUS COATING

I.E. Andzhikovich[1], T.I. Belyankova[1,2*], V.V. Kalinchuk[1,2], G.Yu. Levi[1,2], M.O. Levi[1,2], V.A. Lyzhov[1,2]

[1]Southern Federal University, Bolshaya Sadovaya Str. 105, Rostov-on-Don 344006, Russia

[2]Southern Scientific Center of Russian Academy of Sciences, Chekhov Ave. 41, Rostov-on-Don 344006, Russia

*e-mail: tbelen415@mail.ru

Abstract. Within the framework of a model for the piezoelectric structure with a coating made of a functionally graded material with a piecewise-continuous variation of properties, the problem of propagation of horizontally polarized shear surface waves was investigated. The influence of the polarization vector orientation and the nature of the coating inhomogeneity on the propagation of surface waves in an "acoustically homogeneous" structure was studied.

Keywords: piezoelectric structure, inhomogeneous coating, functionally graded piezoelectric material, piecewise-continuous variation of properties, surface acoustic wave (SAW), SH-waves, Bleustein-Gulyaev waves

1. Introduction

Traditionally, in acoustoelectronic devices (filters, delay lines, etc.) which use surface acoustic waves (SAWs), an increase in the operating frequency band in two ways. The first one is the use of a substrate with a higher sound velocity, and the second is a reduction in the geometric parameters of the planar structure [1]. These methods have their own natural limitations both in terms of wave propagation velocity in the substrate and in the technology of manufacturing the planar structure. An alternative way to increase the operating frequencies is to improve the design of acoustoelectronic devices by using thin films [2-6]. The peculiarity of wave propagation in thin-film structures provides a unique opportunity to double the operating frequency of the converter due to the formation in the film of a periodic domain structure, which effectively excites the second harmonic of the surface wave [7,8]. In the production of other types of acoustoelectronic devices, micro-electro-mechanical systems, sensory devices for various purposes, the multilayer piezoelectric structures are widely used to improve their characteristics [9-17]. This circumstance requires the development of effective methods, software tools and technologies that allow adequately predicting the dynamics of a layered inhomogeneous medium depending on its structure [18-29]. Actively used analytical and numerical-analytical methods [18-24] allow one to study various properties of the propagation and localization of wave fields in layered-inhomogeneous and functionally graded media [19-22], the features of wave field propagation in solids, taking into account the viscosity and porosity of the medium [18], the presence of friction [24] and surface stresses [25]. The method of boundary integral equations [25,26] demonstrates great efficiency in the study of fundamental properties of wave propagation in three-dimensional deformable bodies. In the study of specific materials, instruments and devices, methods of finite element modeling are effectively used [27]. They allow you to take into account the

http://dx.doi.org/10.18720/MPM.4262019_7

complex structure of composites. For the analysis of simple piezoelectric structures, applied methods based on engineering approaches to the calculation of piezoelectric devices are used [28]. In [29], a generalized model of a prestressed ferroelectric structure with an inhomogeneous coating was proposed. On the example of a layered coating, the change in the surface wave field is studied depending on the nature of the initial mechanical influences on the various components of the structure. In [30], the piezoelectric structures with a coating whose properties vary in a piecewise-continuous manner are considered. The influence of the rigidity and the intensity of density change for the inner layer on the structure of the surface wave field and the SAW propagation velocity have been studied. In this paper, we consider a model of piezoelectric structure with an inhomogeneous coating in which the velocity of the bulk shear wave remains constant with depth – a so called model of an "acoustically homogeneous" medium with rigid or malleable interface inclusion inside the coating. The features of the SAW velocities transformation are shown depending on the change in the thickness of the inner malleable or rigid layer of coating. The influence of the orientation of the polarization vectors for the coating and the substrate on the features of SAW propagation is studied in a wide frequency range.

2. Problem formulation

A problem of propagation of SH-waves on the surface of a composite piezoactive medium in the direction of x_1 is considered. The medium is a homogeneous half-space $x_2 \le 0$, $|x_1|, |x_3| \le \infty$ with coating $0 < x_2 \le H$ whose variation of properties is determined:

$$\rho^{(1)} = \rho_0 f_\rho^{(1)}(x_2),\; c_{ij}^{(1)} = c_{ij}^0 f_c^{(1)}(x_2),\; e_{ij}^{(1)} = e_{ij}^0 f_e^{(1)}(x_2),\; \varepsilon_{ij}^{(1)} = \varepsilon_{ij}^0 f_\varepsilon^{(1)}(x_2), \tag{1}$$

where $\rho_0, c_{ij}^0, e_{ij}^0, \varepsilon_{ij}^0$ are the density and the elastic moduli of the «base» material, respectively.

It is assumed that the piezoelectric structure is made on the basis of the 6mm class piezoelectric with the axis of symmetry directed along x_3; the polarization vectors of the half-space and the coating base material either coincide ($e_{15}^0 = e_{15}^{(2)}$), or are oppositely directed ($e_{15}^0 = -e_{15}^{(2)}$). Harmonic oscillations of the medium are induced by the action of a distant source; the mode of oscillations is steady-state; the dynamic process satisfies conditions

$$u_1^{(n)} = u_2^{(n)} = 0, \partial / \partial x_3 = 0, u_k^{(n)} = u_k^{(n)}(x_1, x_2), u_3^{(0)} = 0, k = 3, 4, n = 0,1,2, \tag{2}$$

the superscript separates the vacuum ($n = 0$), the coating ($n = 1$) and the half-space ($n = 2$).

The formulation of boundary problems, the dispersion relation and the results of the investigations are presented in dimensionless parameters [29,30]. The dimensionless frequency $\kappa_{2e} = \omega h / V_{Se}^{(2)}$ ($V_{Se}^{(2)}$ is the velocity of the half-space shear wave with regard to the piezoelectric properties) is used.

Within the framework of the accepted assumptions, the boundary problem on the oscillations of a composite electro-elastic medium with regard to (2) is determined by the equations [29]:

$$\nabla \cdot \mathbf{\Theta}^{(n)} = \rho^{(n)} \ddot{\mathbf{u}}^{(n)}, \quad \nabla \cdot \mathbf{\Delta}^{(n)} = 0, \quad \Delta\varphi^{(0)} = 0 \tag{3}$$

with the boundary conditions:

problem I (denoted by ***"open-case"***) is for the structure with an electrically free surface

$$\mathbf{n} \cdot \mathbf{\Theta}^{(1)}\Big|_{x_2=H} = 0, \tag{4}$$

$$\mathbf{n} \cdot \mathbf{\Delta}^{(1)}\Big|_{x_2=H} = \mathbf{n} \cdot \mathbf{\Delta}^{(0)}\Big|_{x_2=H}, \quad \varphi^{(1)}\Big|_{x_2=H} = \varphi^{(0)}\Big|_{x_2=H}, \tag{5}$$

$$\mathbf{u}^{\mathbf{e}(1)}\Big|_{x_2=0} = \mathbf{u}^{\mathbf{e}(2)}\Big|_{x_2=0}, \; \mathbf{n} \cdot \mathbf{\Theta}^{(1)}\Big|_{x_2=0} = \mathbf{n} \cdot \mathbf{\Theta}^{(2)}\Big|_{x_2=0}, \; \mathbf{n} \cdot \mathbf{\Delta}^{(1)}\Big|_{x_2=0} = \mathbf{n} \cdot \mathbf{\Delta}^{(2)}\Big|_{x_2=0}, \tag{6}$$

$$\mathbf{u}^{\mathbf{e}(2)}\Big|_{x_2 \to -\infty} \to 0, \quad \mathbf{u}^{\mathbf{e}(0)}\Big|_{x_2 \to \infty} \to 0, \tag{7}$$

problem II (denoted by ***"shorted case"***) is for the structure with a metalized surface. In *problem II* the condition

$$\varphi^{(1)}\Big|_{x_2=H}=0 \tag{5a}$$

is used instead of (5).

In (3)–(7) we use the following notations: $\mathbf{u}^{\mathbf{e}(n)}=\left\{u_3^{(n)},u_4^{(n)}=\varphi^{(n)}\right\}$ is the augmented vector of displacements; $\varphi^{(n)}$ is the function of the electrical potential; $\rho^{(n)}$ is the material density of n-th component of the structure; $\boldsymbol{\Theta}^{(n)}$ and $\boldsymbol{\Delta}^{(n)}$ are the stress tensor and the induction vector, respectively; ∇ is Hamilton operator; $\Delta=\partial^2/\partial x_1{}^2+\partial^2/\partial x_2{}^2$ is Laplace operator; $\mathbf{n}$ is the vector of external normal to the surface.

The components of the stress tensor $\boldsymbol{\Theta}^{(n)}$ and induction vector $\boldsymbol{\Delta}^{(n)}$ are:

$$\Theta_{lk}^{(n)}=\theta_{lksp}^{(n)}u_{s,p}^{(n)}+\theta_{lk4p}^{(n)}\varphi_{,p}^{(n)},\ D_l^{(n)}=\theta_{l4sp}^{(n)}u_{s,p}^{(n)}+\theta_{l44p}^{(n)}\varphi_{,p}^{(n)},\quad k,l,s,p=1,2,3, \tag{8}$$

where $\theta_{lksp}^{(n)}=c_{lksp}^{(n)}$, $\theta_{lk4p}^{(n)}=e_{plk}^{(n)}$, $\theta_{l4sp}^{(n)}=e_{lsp}^{(n)}$, $\theta_{l44p}^{(n)}=-\varepsilon_{lp}^{(n)}$; $c_{ij}^{(n)}$, $e_{ij}^{(n)}$, $\varepsilon_{ij}^{(n)}$ – components of tensors of elastic constants, piezoelectric modules and permittivity tensor.

The boundary value problem (3) – (7), taking into account the notation (8), is represented in the form:

$$\begin{aligned}&\sum_{k=1}^{2}\left[\theta_{k33k}^{(1)}u_{3,kk}^{(1)}+\theta_{k34k}^{(1)}u_{4,kk}^{(1)}\right]+\sum_{k=3}^{4}\theta_{23k2}^{(1)}{}'u_{k,2}^{(1)}=\rho_0^{(1)}\frac{\partial^2u_3^{(1)}}{\partial t^2},\\&\sum_{k=1}^{2}\left[\theta_{k43k}^{(1)}u_{3,kk}^{(1)}+\theta_{k44k}^{(1)}u_{4,kk}^{(1)}\right]+\sum_{k=3}^{4}\theta_{24k2}^{(1)}{}'u_{k,2}^{(1)}=0,\end{aligned}\qquad 0<x_2\le H, \tag{9}$$

$$\begin{aligned}&\sum_{k=1}^{2}\left[\theta_{k33k}^{(2)}u_{3,kk}^{(2)}+\theta_{k34k}^{(2)}u_{4,kk}^{(2)}\right]=\rho_0^{(2)}\frac{\partial^2u_3^{(2)}}{\partial t^2},\\&\sum_{k=1}^{2}\left[\theta_{k43k}^{(2)}u_{3,kk}^{(2)}+\theta_{k44k}^{(2)}u_{4,kk}^{(2)}\right]=0,\end{aligned}\qquad x_2\le 0, \tag{10}$$

$$\sum_{k=1}^{2}u_{4,kk}^{(0)}=0,\quad x_2>0. \tag{11}$$

The surface of the medium is free of mechanical stress

$$\Theta_{23}^{(1)}\Big|_{x_2=H}=\sum_{k=3}^{4}\left[\theta_{23k2}^{(1)}u_{k,2}^{(1)}\right]\Big|_{x_2=H}=0. \tag{12}$$

The electrical open conditions at the free surface may be presented as:

$$\begin{aligned}&D_2^{(1)}\Big|_{x_2=H}=\sum_{k=2}^{4}\left[\theta_{24k2}^{(1)}u_{k,2}^{(1)}\right]\Big|_{x_2=H}=D_2^{(0)}\Big|_{x_2=H},\\&u_4^{(1)}\Big|_{x_2=H}=u_4^{(0)}\Big|_{x_2=H}.\end{aligned} \tag{13}$$

The electrical shorted conditions at the free surface are expressed as follows:

$$u_4^{(1)}\Big|_{x_2=H}=0. \tag{14}$$

Along the interfaces between the layer and the substrate, the stresses, mechanical displacements, electrical potentials and electrical displacements are all continuous:

$$\mathbf{u}^{e(1)}\Big|_{x_2=0}=\mathbf{u}^{e(2)}\Big|_{x_2=0},\ \Theta_{23}{}^{(1)}\Big|_{x_2=0}=\Theta_{23}{}^{(2)}\Big|_{x_2=0},\ D_2{}^{(1)}\Big|_{x_2=0}=D_2{}^{(2)}\Big|_{x_2=0}. \tag{15}$$

Conditions at the infinity have the form:

$$\mathbf{u}^{\mathbf{e}(2)}\Big|_{x_2\to-\infty}\to 0,\quad \mathbf{u}^{\mathbf{e}(0)}\Big|_{x_2\to\infty}\to 0. \tag{16}$$

In Fourier transforms, the dispersion equation of *problems I* and *II* for a piezoelectric structure with a functionally graded coating can be represented in the same form as in [29] (further α is the transformation parameter by coordinate x_1):

$$\det\begin{pmatrix} \mathbf{B}^{(1)}(H) & \mathbf{G}^{(1)} \\ \mathbf{A}^{(1)}(0) & \mathbf{B}^{(2)}(0) \end{pmatrix} = 0. \tag{17}$$

Matrices-elements of dispersion equation (17) are obtained by satisfying the boundary conditions (12)–(16) of system (9)–(11) solutions for homogeneous and inhomogeneous components of the structure. For a homogeneous piezoelectric half-space we use a traditional analytical representation of the solution by means of the expansion in terms of exponentials; matrix $\mathbf{B}^{(2)}(0)$ is determined by the properties of the half-space and by the conditions (15), (16). The general solution for inhomogeneous coating (9) [29] is given by means of the expansion in terms of $y_{kp}^{(1)}(\alpha, x_2)$ which are linearly independent solutions of Cauchy problem for equations

$$\mathbf{Y}^{(1)\prime} = \mathbf{M}^{(1)}(\alpha, x_2)\mathbf{Y}^{(1)},\ \mathbf{Y}^{(1)} = \begin{pmatrix} \mathbf{Y}_\Sigma^1 \\ \mathbf{Y}_\mathbf{u}^1 \end{pmatrix},\ \mathbf{Y}_\Sigma^1 = \begin{pmatrix} \Theta_{23}^{F(1)} \\ D_2^{F(1)} \end{pmatrix},\ \mathbf{Y}_\mathbf{u}^1 = \begin{pmatrix} U_3^{(1)} \\ U_4^{(1)} \end{pmatrix}, \tag{18}$$

$$\mathbf{M}^{(1)}(\alpha, x_2) = \begin{pmatrix} 0 & 0 & \alpha^2\theta_{1331}^{(1)} - \rho^{(1)}\kappa_2^2 & \alpha^2\theta_{1431}^{(1)} \\ 0 & 0 & \alpha^2\theta_{1431}^{(1)} & \alpha^2\theta_{1441}^{(1)} \\ -\theta_{2442}^{(1)}(g_0)^{-1} & \theta_{2432}^{(1)}(g_0)^{-1} & 0 & 0 \\ \theta_{2432}^{(1)}(g_0)^{-1} & -\theta_{2332}^{(1)}(g_0)^{-1} & 0 & 0 \end{pmatrix}, \tag{19}$$

$$g_0 = \theta_{2442}^{(1)}\theta_{2332}^{(1)} - \left(\theta_{2432}^{(1)}\right)^2$$

with initial conditions $y_{kp}^{(1)}(\alpha, 0) = \delta_{kp}$. Here $\Theta_{23}^{F(n)}, D_2^{F(n)}, U_k^{(n)}$ are Fourier transforms of the components of the stress tensor, the induction vector and the augmented vector of displacements, respectively; δ_{kp} is Kronecker delta. The solution of system (18)–(19) is possible by using different numerical methods; in this paper we use the modification of Runge-Kutta method.

Matrix $\mathbf{B}^{(1)}(H)$ is determined by the coating parameters and the conditions (12), (13) (open-case) or (12), (14) (shorted-case). Matrix $\mathbf{A}^{(1)}(0)$, with regard to the initial conditions of Cauchy problem, is the identity matrix $\mathbf{A}^{(1)}(0) = \mathbf{E}$. In open-case

$$\mathbf{B}^{(1)}(H) = \begin{pmatrix} y_{11}^{(1)} & y_{12}^{(1)} & y_{13}^{(1)} & y_{14}^{(1)} \\ y_{21}^{(1)}\gamma & y_{22}^{(1)}\gamma & y_{23}^{(1)}\gamma & y_{24}^{(1)}\gamma \\ y_{41}^{(1)}\gamma & y_{42}^{(1)}\gamma & y_{43}^{(1)}\gamma & y_{44}^{(1)}\gamma \end{pmatrix},\ \mathbf{G}^{(1)} = \begin{pmatrix} 0 & 0 & 0 \\ 0 & 0 & -\varepsilon^{(0)}\alpha \\ 0 & 0 & -1 \end{pmatrix},\ \mathbf{B}^{(2)}(0) = \begin{pmatrix} -l_{11}^2 & -l_{12}^2 & 0 \\ -l_{21}^2 & -l_{22}^2 & 0 \\ -f_{31}^2 & -f_{32}^2 & 0 \\ -f_{41}^2 & -f_{42}^2 & 0 \end{pmatrix},$$

$$\gamma = e^{\alpha H},\quad f_{41}^2 = \theta_{2432}^{(2)} / \theta_{2442}^{(2)},\ f_{31}^2 = f_{42}^2 = 1,\ f_{32}^2 = 0,$$

$$l_{pk}^2 = \sigma_k^{(2)} l_{pk}^{2*},\quad l_{1k}^{2*} = \theta_{2332}^{(2)} f_{3k}^2 + \theta_{2342}^{(2)} f_{4k}^2,\quad l_{2k}^{2*} = \theta_{2432}^{(2)} f_{3k}^2 + \theta_{2442}^{(2)} f_{4k}^2. \tag{20}$$

Here the coefficients $\sigma_k^{(2)}$ satisfy the characteristic equation

$$\det \mathbf{M}_\sigma^{(2)}(r) = 0,\ \mathbf{M}_\sigma^{(2)}(r) = \begin{pmatrix} \theta_{2332}^{(2)} r^2 - \left(\alpha^2\theta_{1331}^{(2)} - \rho^{(2)}\kappa_2^2\right) & \theta_{2342}^{(2)} r^2 - \alpha^2\theta_{1341}^{(2)} \\ \theta_{2432}^{(2)} r^2 - \alpha^2\theta_{1431}^{(2)} & \theta_{2442}^{(2)} r^2 - \alpha^2\theta_{1441}^{(2)} \end{pmatrix}. \tag{21}$$

The coefficients f_{pk}^2 are determined from the solution of a homogeneous system of linear equations with a matrix $\mathbf{M}_\sigma^{(2)}\left(\sigma_k^{(2)}\right)$. In shorted-case the matrix $\mathbf{B}^{(1)}\left(H\right)$, $\mathbf{B}^{(2)}\left(0\right)$ and $\mathbf{G}^{(1)}$ have dimension 2×4, 4×2 and 2×2 respectively

$$\mathbf{B}^{(1)}\left(H\right)=\begin{pmatrix} y_{11}^{(1)} & y_{12}^{(1)} & y_{13}^{(1)} & y_{14}^{(1)} \\ y_{41}^{(1)} & y_{42}^{(1)} & y_{43}^{(1)} & y_{44}^{(1)} \end{pmatrix},\ \mathbf{G}^{(1)}=0,\ \mathbf{B}^{(2)}\left(0\right)=\begin{pmatrix} -l_{11}^2 & -l_{12}^2 \\ -l_{21}^2 & -l_{22}^2 \\ -f_{31}^2 & -f_{32}^2 \\ -f_{41}^2 & -f_{42}^2 \end{pmatrix}. \tag{22}$$

3. Numerical analysis

The investigations were carried out for the piezoelectric structures made from the ferroelectric material with parameters [1]: $\rho=5680\,kg/m^3$, $V_P=6097\,m/s$, $V_S=2743\,m/s$, $V_{Se}=2892\,m/s$, $V_{GB}^f/V_{Se}=0.999947$, $V_{GB}^m/V_{Se}=0.994944$. We assumed that the structure was an "acoustically homogeneous" medium, i.e., with regard to (1) $f_s^{(1)}\left(x_2\right)=f^{(1)}\left(x_2\right)$ ($s=\rho=c=e=\varepsilon$). The physical properties of the coating change in a piecewise-continuous manner: the coating is divided into M components with constant parameters: $f_s^{(1)}\left(x_2\right)=f_s^{(1_k)}\Big|_{x_2\in[h_k,\mathrm{h}_{k+1}]}$ $k=1,2,...M$. Further, we considered the two types of coating. M =2 corresponds to a two-layer coating, where the internal layer simulates the compliant ($\gamma^2=f^{(1_2)}/f^{(2)}<1$) or rigid ($\gamma^2>1$) inclusion, its thickness is h_2. The outer layer has half-space properties ($\gamma^1=f^{(1_1)}/f^{(2)}=1$), its thickness is H-h_2. $M=1$ corresponds to the one-layer soft ($\gamma=f^{(1)}/f^{(2)}=0.1$) or rigid ($\gamma=5$) coating.

In Figures 1a,b we showed the influence of the internal layer thickness h_2 and its rigidity on the SAW velocities ($V_F^{(1)}/V_{Se}^{(2)}$, where $V_F=\kappa_2/\xi$, ξ is the solution of equation (17) with the notation (20), (21) for *problem I* or (22) for *problem II*) for the structure with a two-layer coating in shorted-case if $e_{15}^0=e_{15}^{(2)}$. Curves 1, 2, …, 10 (Fig. 1*a*) correspond to the increase of thickness $h_2=$ 0.1, 0.3, 0.5, 0.7, 0.9, 0.96, 0.98, 0.99, 0.996, 0.999 if $\gamma^2=0.1$, curves 1, 2,…, 7 (Fig. 1b) correspond to $h_2=$ 0.2, 0.4, 0.6, 0.8, 0.9, 0.96, 0.99 for $\gamma^2=5$. Number 0 denotes the SAW velocities for the structures with one-layer coating ($\gamma=0.1$ corresponds to Fig. 1*a*, $\gamma=5$ corresponds to Fig. 1*b*).

Based on the graphs, thickness of the inclusion has a significant effect on the phase velocity of SAW. In the case $\gamma=5$ (hard inclusion), the influence of the thickness of the inner layer is localized in the low-frequency range. At the low frequencies, there is a decrease in phase velocity, which is greater, when the greater the thickness of the inner layer. Having reached a minimum, the phase velocity begins to increase to a value enclosed in the interval $\left[V_{GB}^m,V_{Se}^{(2)}\right]$. The greater this interval, the smaller the thickness of the inner layer.

In the case of compliant inclusion, the range of influence of the thickness on the phase velocity substantially increases both in frequency and in amplitude. In this case, the behavior of the velocity in the asymptotics remains less than the velocity V_{GB}^m

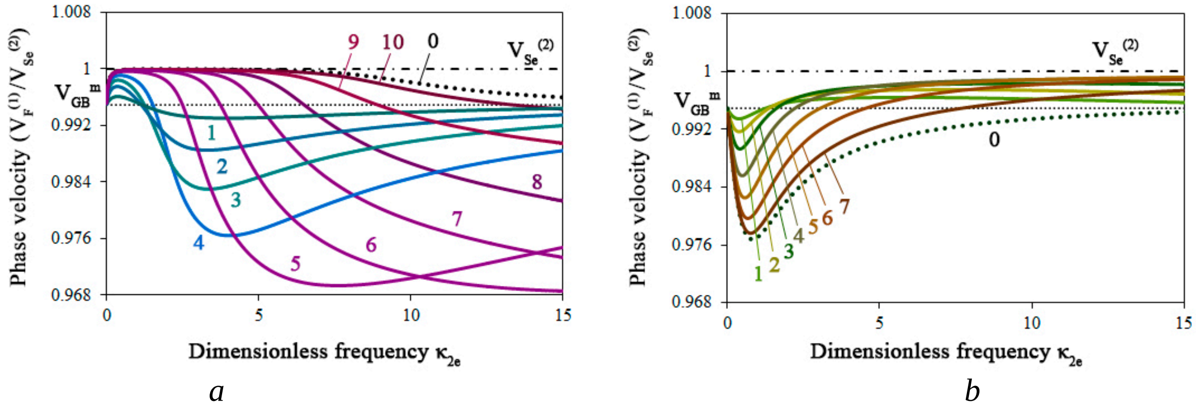

Fig. 1. Influence of the thickness of the coating internal layer on SAW velocities. Problem II. $\gamma^1 = 1, e_{15}^0 = e_{15}^{(2)}$, a) $\gamma^2 = 0.1$, b) $\gamma^2 = 5$

Further, we consider a two-layer coating in which the thickness of the inner layer is h_2=0.5H. Figure 2a–d illustrates the influence of the polarization vector orientation for the coating and the substructure ($e_{15}^{(2)} = e_{15}^0$ – Fig. 2a, b; $e_{15}^{(2)} = -e_{15}^0$ – Fig. 2c, d) on the SAW velocities in case of a compliant (Fig. 2a, c) and a rigid (Fig. 2b, d) internal layer. Numbers 1, 2,…,7 in Fig. 2a,c denote the curves for $\gamma^2 = 0.8$, 0.6, 0.5, 0.4, 0.3, 0.2, 0.1; curves 1, 2,…, 5 in Fig. 2c,d correspond to $\gamma^2 =$ 2, 3, 5, 8, 10; number 0 denotes Bleustein–Gulyaev waves (BGW) in problem II (shorted case, $\gamma^2 = \gamma^1 = 1, \quad e_{15}^{(2)} = -e_{15}^0$).

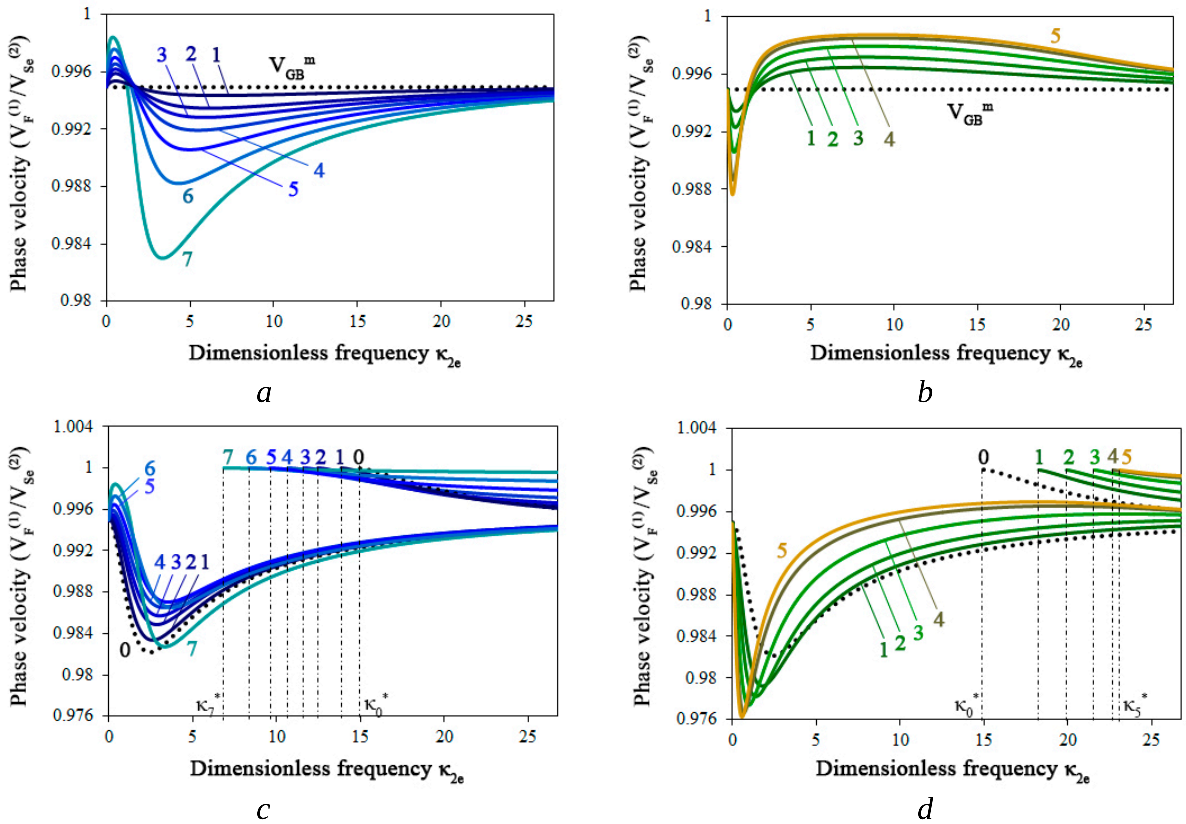

Fig. 2. Influence of the polarization vector orientation for the coating and the substructure on SAW velocities. Problem II; *M*=2, h_2=0.5; a, b) $e_{15}^0 = e_{15}^{(2)}$; c, d) $e_{15}^0 = -e_{15}^{(2)}$

As follows from the graphs, the direction of polarization has a significant effect on the speed of the SAW. With coaxial polarization of the coating and substrate, the SAW phase velocity in the coating with compliant inclusion increases first, then decreases sharply. Having reached a minimum, the speed of the SAW begins to increase. In the limit at high frequencies, the velocity asymptotically approaches the velocity of the BGW from below. In a coating with a hard inclusion, the speed first decreases, then increases sharply. Having reached its maximum value, it begins to decrease. In the limit at high frequencies, it asymptotically approaches the BGW velocity from above.

With opposite polarization of the coating and the substrate, the behavior of surfactants for different coatings is qualitatively identical. The main feature is the presence of a second mode, the frequency of occurrence of which depends on the value of the stiffness or ductility of the inclusion. The difference is only quantitative.

Figures 3*a*,*b* show the frequency dependences of SAW velocities for a structure with a free surface (problem I) in case of a compliant (Fig. 3*a*) and a rigid (Fig. 3*b*) internal layer of the coating. Numbers 1, 2,…,7 (Fig. 3.*a*) and 1,2,…,5 (Fig. 3.*b*) denote the curves corresponding to the values of γ^2 in Fig. 2; number 0 in Fig. 3 denotes BGW of problem I ($\gamma^2 = \gamma^1 = 1$, $e_{15}^0 = -e_{15}^{(2)}$).

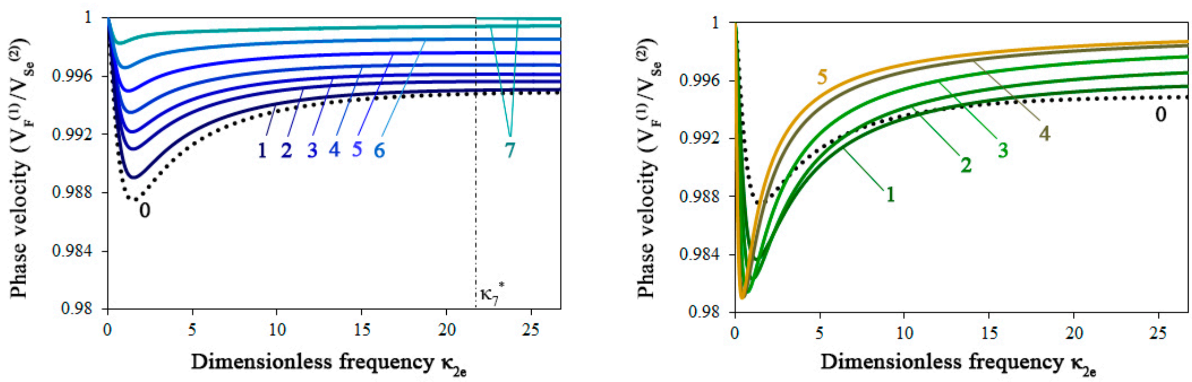

a *b*

Fig. 3. Influence of the rigidity of the coating internal layer on SAW velocities. Problem I; M =2, h$_2$=0.5, $e_{15}^0 = -e_{15}^{(2)}$; a) $\gamma^2 < 1$; b) $\gamma^2 > 1$

As follows from the graphs, hard switching is characterized by a significant gradient at low frequencies. Compliant inclusion is distinguished by a more significant differentiation of the values of the SAW velocity at high frequencies.

4. Conclusion

A model is constructed that allows one to study the process of formation of wave fields in a piezoelectric structure with an inhomogeneous coating. The model is based on the reduction of a boundary value problem for a partial differential equation to a system of Cauchy problems with initial conditions. The solution of the latter is built numerically. As an example, the features of the SAW propagation on the surface of a structure with an inhomogeneous coating, in which the velocity of the shear bulk wave is constant in thickness, are studied. The cases of hard and compliant inclusions are considered, the features of the influence of the coating thickness, the direction of its polarization on the phase velocity of the SAW are investigated. The possibility of controlling the structure of the wave field on the surface of the medium by changing the physical properties and geometric parameters of the coating is shown.

Acknowledgements. *The work was supported by the Ministry of Education and Science of Russia, competitive part of state assignment, No. 9.1001.2017/ 4.6 and partially by the Russian Foundation for Basic Research (projects 19-08-01051, 19-48-230042, 19-01-00719 and 18-08-01012).*

References

[1] Matthews H. *Surface Wave Filters. Design, Construction and use.* New York: John Wiley & Sons; 1977.

[2] Emanetoglu N, Gorla C, Liu Y, Liang S, Lu Y. Epitaxial ZnO piezoelectric thin films for saw filters. *Materials Science in Semiconductor Processing.* 1999;2(3): 247-252.

[3] Omori T, Hashimoto K, Yamaguchi M. PZT thin films for SAW and BAW devices. In: *Proc. Int'l Symp. on Acoustic Wave Devices for Future Mobile Comm. Systems*. 2001: p.245-250.

[4] Kirby P, Su QX, Komuro E, Imura M, Zhang Q, Whatmore R. High frequency thin film ferroelectric acoustic resonators and filters. *Integrated Ferroelectrics: An International Journal.* 2001;41(1–4): 91–100.

[5] Salut R, Daniau W, Ballandras S, Gariglio S, Triscone G, Triscone JM. P1H-3 Epitaxial Pb(Zr0.2Ti0.8)O3 Thin Layers for the Fabrication of RadioFrequency Elastic Wave Transducers. In: *2007 IEEE Ultrasonics Symposium Proceedings.* Piscataway: Institute of Electrical and Electronics Engineers; 2007. p.1421-1424

[6] Khassaf H, Khakpash N, Sun F, Sbrockey NM, Tompa GS, Kalkur TS, Alpay SP. Strain engineered barium strontium titanate for tunable thin film resonators. *Appl. Phys. Lett.* 2014;104(20): 202902.

[7] Mukhortov VM, Biryukov SV, Golovko YI, Karapet'yan GY, Masychev SI, Mukhortov VM. Surface Acoustic Waves in Thin Films of Barium Strontium Titanate on Magnesium Oxide Substrates. *Technical Physics Letters*. 2011;37(5): 207-209.

[8] Biryukov SV, Golovko YI, Masychev SI, Mukhortov VM. Surface acoustic waves converters with electrically adjustable sensitivity. *Science of the south of Russia*. 2016;12(1): 11-15. (In Russian)

[9] Li XY, Wang ZK, Huang SH. Love waves in functionally graded piezoelectric materials. *Intern. J. Solids and Struct.* 2004;41(26): 7309-7328.

[10] Liu J, Wang ZK. The propagation behavior of Love waves in a functionally graded layered piezoelectric structure. *Smart Mater. Struct.* 2005;14(1): 137-146.

[11] Liu JX, Fang DN, Wei WY, Zhao XF. Love waves in layered piezoelectric/piezomagnetic structures. *Journal of Sound and Vibration*. 2008;315(1-2): 146-156.

[12] Qian ZH, Jin F, Lu T, Kishimoto K. Transverse surface waves in a layered structure with a functionally graded piezoelectric substrate and a hard dielectric layer. *Ultrasonics.* 2009;49(3): 293-297.

[13] Belyankova TI, Kalinchuk VV, Lyzhov VA. A coupled mixed problem for a system of electrodes on the surface of a prestressed electroelastic structurally inhomogeneous half-space. *Journal of Applied Mathematics and Mechanics*. 2010;74(6): 637-647.

[14] Qian ZH, Jin F, Hirose S. Dispersion characteristics of transverse surface waves in piezoelectric coupled solid media with hard metal interlayer. *Ultrasonics*. 2011;51(8): 853-856.

[15] Majhi S, Pal PC, Kumar S. Love waves in a layered functionally graded piezoelectric structure under initial stress. *Waves in Random and Complex Media.* 2016;26(4): 535-552.

[16] Guo X, Wei P, Li L, Lan M. Effects of functionally graded interlayers on dispersion relations of shear horizontal waves in layered piezoelectric/piezomagnetic cylinders. *Applied Mathematical Modelling.* 2018;55: 569-582.

[17] Huan Q, Chen M, Su Z, Li F. A high-resolution structural health monitoring system based on SH wave piezoelectric transducers phased array. *Ultrasonics.* 2019;97: 29-37.
[18] Igumnov LA, Amenitskii AV, Belov AA, Litvinchuk SY, Petrov AN. Numerical-analytic investigation of the dynamics of viscoelastic and porous elastic bodies. *Journal of Applied Mechanics and Technical Physics*. 2014;55(1): 89-94.
[19] Belyankova TI, Kalinchuk VV. On the problem of analyzing the dynamic properties of a layered half-space. *Acoustical Physics*. 2014;5: 530-542.
[20] Belyankova TI, Kalinchuk VV. Peculiarities of the wave field localization in the functionally graded layer. *Materials Physics and Mechanics.* 2015;23(1): 25-30.
[21] Kausel E. Generalized stiffness matrix method for layered soils. *Soil Dynamics and Earthquake Engineering.* 2018;115: 663-672.
[22] Bednarik M, Cervenka M, Lotton P, Simon L. Analytical solutions for elastic SH-waves propagating through an isotropic inhomogeneous layer. *Composite Structures.* 2019;220: 875-887.
[23] Li P, Shan S, Wen F, Cheng L. A fully-coupled dynamic model for the fundamental shear horizontal wave generation in a PZT activated SHM system. *Mechanical Systems and Signal Processing.* 2019;116: 916-932.
[24] Kirillova EV, Seemann W, Shevtsova MS. The influence of an adhesive layer on the interaction between a piezo-actuator and an elastic 3D-layer and on the excited wave fields. *Materials Physics and Mechanics.* 2019:42(1): 40-53.
[25] Eremeyev VA, Rosi G, Naili S. Comparison of anti-plane surface waves in strain-gradient materials and materials with surface stresses. *Mathematics and Mechanics of Solids.* 2019;24(8): 2526-2535
[25] Igumnov LA. Boundary integral equations for three-dimensional problems on plane waves. *Doklady Physics.* 2006;51(8): 440-443.
[26] Igumnov LA, Markov IP, Boev AV. Boundary element time-harmonic analysis of 3D linear piezoelectric solids. *Materials Physics and Mechanics.* 2019;42(2): 256-264.
[27] Iovane G, Nasedkin AV. Finite element modelling of ceramomatrix piezocomposites by using effective moduli method with different variants of boundary conditions. *Materials Physics and Mechanics*. 2019:42(1): 1-13.
[28] Soloviev AN, Chebanenko VA, Parinov IA, Oganesyan PA. Applied theory of bending vibrations of a piezoelectric bimorphwith a quadratic electric potential distribution. *Materials Physics and Mechanics*. 2019:42(1): 65-73.
[29] Belyankova TI, Kalinchuk VV. Surface sh-waves in pre-stressed piezoelectrics with functionally graded coating. *PNRPU Mechanics Bulletin*. 2016;3: 7-27.
[30] Belyankova TI, Kalinchuk VV. Modeling of prestressed piezoelectric structures with inhomogeneous coating. *Procedia Engineering.* 2017;199: 1513-1518.